

# All-vacuum deposited perovskite solar cells with glycine modified NiO<sub>x</sub> hole-transport layer

Cheng Fang<sup>a</sup>, Qianqian Zhao<sup>a</sup>, Fuping Zhao<sup>a</sup>, Fuzhi Huang<sup>a,b</sup>, Yong Peng<sup>a</sup>,  
Zhiliang Ku<sup>\*a,b</sup>, Yi-Bing Cheng<sup>b</sup> and Zhengyi Fu<sup>\*a</sup>

<sup>a</sup>State Key Laboratory of Advanced Technologies for Materials Synthesis and Processing, Wuhan University of Technology, 122 Luoshi Road, Wuhan 430070, Hubei Province, China

<sup>b</sup>Foshan Xianhu Laboratory of the Advanced Energy Science and Technology Guangdong Laboratory, Foshan 528216, Guangdong Province, China

\*Corresponding author: Zhiliang Ku, E-mail: [zhiliang.ku@whut.edu.cn](mailto:zhiliang.ku@whut.edu.cn); Zhengyi Fu, E-mail: [zyfu@whut.edu.cn](mailto:zyfu@whut.edu.cn)

**Keywords:** All-vacuum deposition; perovskite solar cell; nickel oxide; glycine

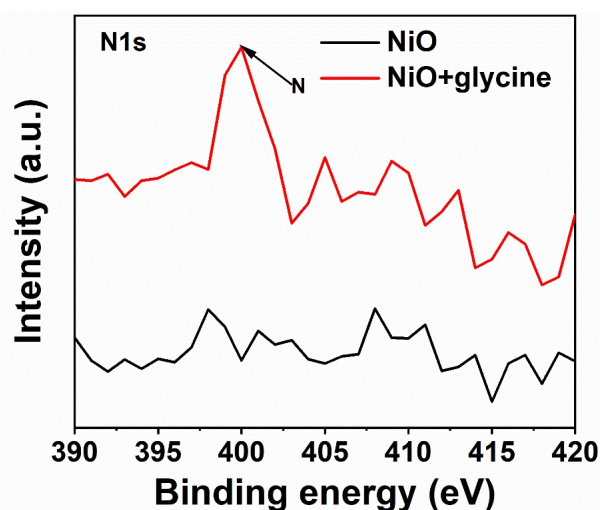


**Figure S1.** XPS high resolution spectra of the N1s.

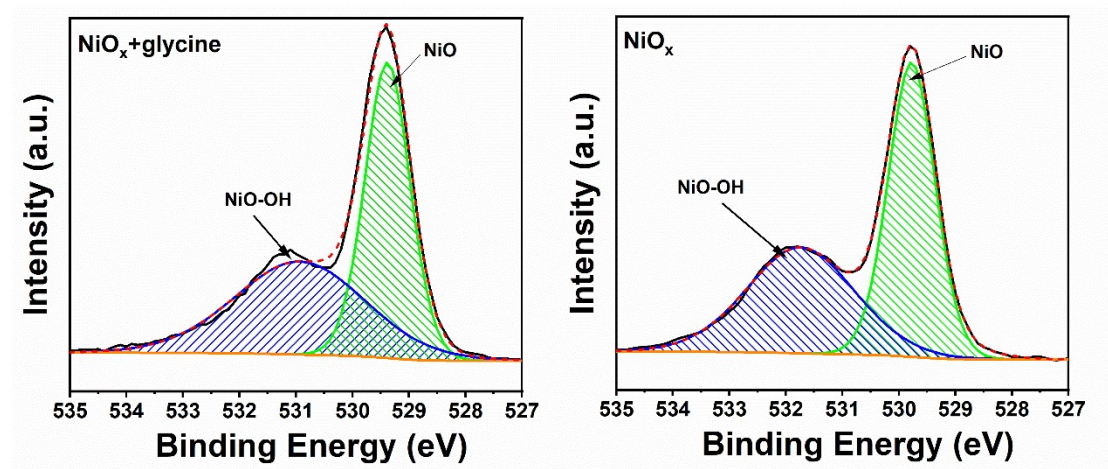


**Figure S2.** XPS spectra of O1s peak for NiO<sub>x</sub>+glycine and NiO<sub>x</sub> films.

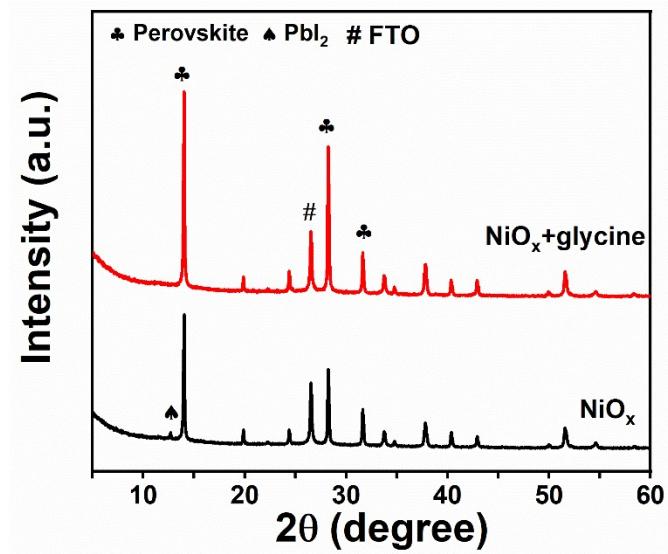


**Figure S3.** XRD patterns of perovskite films grown on NiO<sub>x</sub>+glycine and NiO<sub>x</sub> films.

**Table S1.** Contact angles of the NiO<sub>x</sub> films with different immersion time in glycine solution.

Immersion time (min)	Contact angle (°)	
	left	right
0	23.75	21.33
30	32.86	32.66
60	47.22	47.91
90	69.70	63.93
120	69.61	67.94
150	67.81	65.55

**Table S2.** Fitted parameters of the TRPL spectra.

Substrate	A <sub>1</sub>	τ <sub>1</sub> (ns)	A <sub>2</sub>	τ <sub>2</sub> (ns)
NiO <sub>x</sub>	526	58	756	174
NiO <sub>x</sub> +glycine	332	37	933	214

**Table S3.** PCE of devices based on different preparation methods and modified materials

HTL					
Deposition Routes	Perovskite	Treatment of materials	PCE%(w/w)	Year	Ref
sol-gel	$\text{CH}_3\text{NH}_3\text{PbI}_{3-x}\text{Cl}_x$	Ethanolamine molecules (EDA)	15.70/11.47	2016	[1]
Spin $\text{NiO}_x$ NPs	$\text{MAPbI}_3$	para-substituted benzoic acid	18.4/15.3	2017	[2]
Solution( $\text{Cu}:\text{NiO}_x$ )	$\text{MAPbI}_3$	Cysteine (Cys)	17.8/14.4	2018	[3]
Solution	$\text{MAPbI}_3$	n-Butylamine	18.9/13.2	2019	[4]
Solution	CsFAMA mixed	2,2'-bipyridine(/2,2'-BiPy)	15.86/16.53	2019	[5]
Sputter	$\text{Cs}_{0.05}(\text{FA}_{0.83}\text{MA}_{0.17})_{0.9}$ ${}_5\text{Pb}(\text{I}_{0.82}\text{Br}_{0.18})_3$	[2-(3,6-dimethoxy-9H-carbazol-9-yl)ethyl]phosphonic acid (MeO-2PACz)	19.9/17.9	2021	[6]
Spin-coating $\text{NiO}_x$ NPs	CsFAMA mixed	3-(Triethoxysilyl)propylamine (TSPA)	20.21/18.71	2021	[7]
spin-coating $\text{NiO}_x$ NPs	$\text{MAPbI}_3$	trimethylolpropane tris(2-methyl-1-aziridinepropionate) (SaC-100)	19.29/17.54	2021	[8]
Sputter	$\text{Cs}_{0.05}\text{MA}_{0.15}\text{FA}_{0.80}\text{Pb}(\text{I}_{0.85}\text{Br}_{0.15})_3$	organometallic dye molecule (N719)	19.2/16.7	2021	[9]
Sputter	$\text{MAPbI}_3$	\	15.7	2021	[10]
Sputter	$\text{MAPbI}_3$	\	15.6	2021	[11]
E-beam	$\text{MAPbI}_3$	\	15.4	2018	[12]
E-beam	$\text{MAPbI}_3$ (Co-evaporation)	\	15.6	2019	[13]
E-beam	$\text{Cs}_{0.14}\text{FA}_{0.86}\text{Pb}(\text{Br}_x\text{I}_{1-x})_3$ (Vapor-solid reaction)	glycine	17.96/15.27	2022	This work

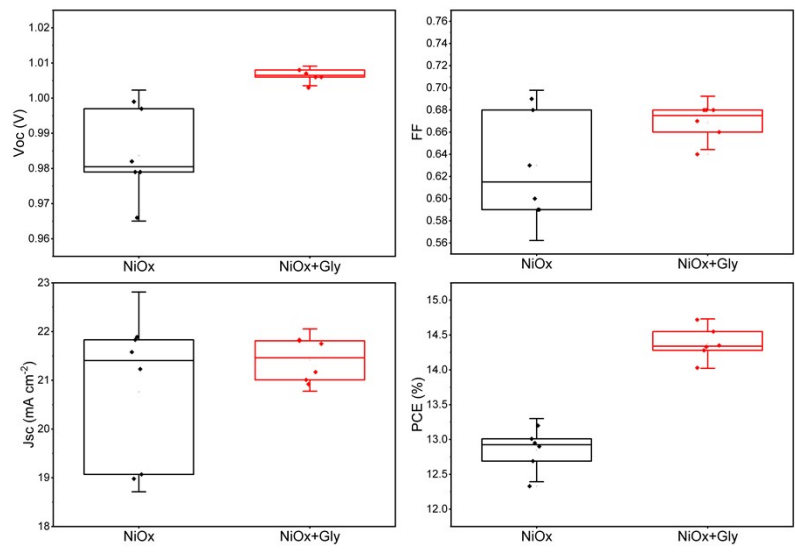


Fig S4. Statistical results of the  $J$ - $V$  parameters of devices based on NiO<sub>x</sub> and NiO<sub>x</sub>+glycine films.

## Reference

- [1] Y. Bai, H. Chen, S. Xiao, Q. Xue, T. Zhang, Z. Zhu, Q. Li, C. Hu, Y. Yang, Z. Hu, F. Huang, K. S. Wong, H.-L. Yip, S. Yang, *Advanced Functional Materials* **2016**, 26, 2950.
- [2] Q. Wang, C. C. Chueh, T. Zhao, J. Cheng, M. Eslamian, W. C. H. Choy, A. K. Jen, *ChemSusChem* **2017**, 10, 3794.
- [3] J. He, Y. Xiang, F. Zhang, J. Lian, R. Hu, P. Zeng, J. Song, J. Qu, *Nano Energy* **2018**, 45, 471.
- [4] Y. Cheng, M. Li, X. Liu, S. H. Cheung, H. T. Chandran, H.-W. Li, X. Xu, Y.-M. Xie, S. K. So, H.-L. Yip, S.-W. Tsang, *Nano Energy* **2019**, 61, 496.
- [5] Y.-W. Zhang, P.-P. Cheng, J.-M. Liang, W.-Y. Tan, Y. Min, *Synthetic Metals* **2019**, 258, 116197.
- [6] J. Sun, C. Shou, J. Sun, X. Wang, Z. Yang, Y. Chen, J. Wu, W. Yang, H. Long, Z. Ying, X. Yang, J. Sheng, B. Yan, J. Ye, *Solar RRL* **2021**, 5, 2100663.
- [7] D. S. Mann, P. Patil, S.-N. Kwon, S.-I. Na, *Applied Surface Science* **2021**, 560, 149973.
- [8] J. Zhang, J. Long, Z. Huang, J. Yang, X. Li, R. Dai, W. Sheng, L. Tan, Y. Chen, *Chemical Engineering Journal* **2021**, 426, 131357.
- [9] S. Zhumagali, F. H. Isikgor, P. Maity, J. Yin, E. Ugur, M. De Bastiani, A. S. Subbiah, A. J. Mirabelli, R. Azmi, G. T. Harrison, J. Troughton, E. Aydin, J. Liu, T. Allen, A. u. Rehman, D. Baran, O. F. Mohammed, S. De Wolf, *Advanced Energy Materials* **2021**, 11, 2101662.
- [10] N. Pant, A. Kulkarni, M. Yanagida, Y. Shirai, S. Yashiro, M. Sumiya, T. Miyasaka, K. Miyano, *ACS Applied Energy Materials* **2021**, 4, 4530.
- [11] H.-J. Seok, J.-H. Park, A. Yi, H. Lee, J. Kang, H. J. Kim, H.-K. Kim, *ACS Applied Energy Materials* **2021**, 4, 5452.
- [12] S. R. Pae, S. Byun, J. Kim, M. Kim, I. Gereige, B. Shin, *ACS Appl Mater Interfaces* **2018**, 10, 534.
- [13] T. Abzieher, S. Moghadamzadeh, F. Schackmar, H. Eggers, F. Sutterlütli, A. Farooq, D. Kojda, K. Habicht, R. Schmager, A. Mertens, R. Azmi, L. Klohr, J. A. Schwenzler, M. Hetterich, U. Lemmer, B. S. Richards, M. Powalla, U. W. Paetzold, *Advanced Energy Materials* **2019**, 9, 1802995.